International Journal of Mass Spectrometry 273 (2008) 48–52

Contents lists available at ScienceDirect

International Journal of Mass Spectrometry

journal homepage: www.elsevier.com/locate/ijms

Fragmentation of molecular tributyltin chloride

S. Osmekhin[a,*], A. Caló[a], V. Kisand[b], E. Nõmmiste[b], H. Kotilainen[c], H. Aksela[a], S. Aksela[a]

[a] Department of Physical Sciences, University of Oulu, P.O. Box 3000, FIN-90014, Finland
[b] Institute of Physics, University of Tartu, Riia 142, 51014 Tartu, Estonia
[c] Southwest Finland Regional Environment Center, P.O. Box 47, Turku FIN-20801, Finland

ARTICLE INFO

Article history:
Received 23 January 2008
Received in revised form 18 February 2008
Accepted 19 February 2008
Available online 4 March 2008

Keywords:
Tributyltin
TBTCl
Molecular fragmentation

ABSTRACT

Fragmentation of tributyltin chloride (TBTCl) vapour has been studied experimentally by means of time-of-flight mass spectrometry at the photon energy range of 9–25 eV of synchrotron radiation, at 21.22 eV of HeI as well as with 500 eV electron beam excitation. Branching ratios of the tributyltin chloride fragments taken with HeI and synchrotron radiation have been presented first time. Calculations based on density functional theory (DFT) were carried out for TBTCl and the ionization energies obtained were used to predict the dissociation pathways creating the observed ions.

1. Introduction

Tributyltin (TBT) compounds were first used in the 1960s as an antifouling agent in marine paints. Environmentaly harmful effect of trisubstituted organotins was discovered in the end of the 1970s and TBT compounds have been included on the European Economic Community Priority Pollutants List, but ogranotins are still in use all over the world in different applications [1–4]. In an organotin compound, one or more organic substituent like methyl, ethyl or butyl is attached to tin atom with a covalent bond. Organotins like tributyltin chloride which are trisubstituted R_3SnX (R = for example butyl, X = halogen) have usually higher toxicity than mono- or disubstituted organotin compounds. The anion X has minor influence on the toxicity of trisubstituted organotins, if the X itself is not toxic [1,5,6]. In synthesis of organotin chlorides the first step is to manufacture R_3SnCl, R_2SnCl_2 or $RSnCl_3$ from which various Sn derivatives can simply be produced. TBTCl itself is widely used in antifouling paints, agrochemicals and other applications [1]. Physical properties of water and sediments as well as natural external action were found to define the life-time of the organotins in the systems [7]. The primary natural external action on the system is sunlight, which photolysis of TBTs in natural water was reported to be fairly slow ($t_{1/2} > 89$ days) [8].

In order to evaluate the environmental distribution and fate of organotin compounds in marine environment (in particular water, sediment and sea animals), various analytical methods have been used. These include atomic absorption and emission spectroscopies and electron ionization mass spectroscopies [9–13]. All these methods are based on an interaction between the compound and the photons or electrons. Dissociation created by interaction has an effect to the results obtained, making the data produced hardly comparable.

In present work we study how radiation by photons and electrons influences the dissociation of TBTCl molecule to smaller, less toxic fragments. Clean TBTCl was selected to be the topic of our study as it is typically used as reference reagent for environmental studies. The dissociation was induced by a tuneable monochromatic synchrotron light from MAX-I at the energy range of 9–25 eV. In addition, TBTCl molecules were irradiated by photons from a HeI lamp (with photon energy 21.22 eV) and by electrons with energy of 500 eV. Depending on the energy of the radiation used, ionization/excitation of an electron from a bonding orbital may take place, resulting in breaking the bond. The different ions created as a product of the exposion of TBTCl were detected by a time-of-flight (TOF) mass spectrometer which separates the masses and charges of the ions on the basis of the flight times. The fragmentation of the TBTCl molecule detected strongly depends on the energy of the radiation as will be shown below. To understand the results they were compared with calculations carried out using the DFT approach which predict the ionization energies of different orbitals.

2. Experiment

The experiments with synchrotron radiation were carried out at the bending magnet beam line 52 at the 550 MeV MAX-I storage ring at Lund, Sweden. The radiation is dispersed by a 1 m nor-

* Corresponding author. Tel.: +358 8 553 1317; fax: +358 8 553 1287.
E-mail address: Sergey.Osmekhin@oulu.fi (S. Osmekhin).

1387-3806/$ – see front matter © 2008 Elsevier B.V. All rights reserved.
doi:10.1016/j.ijms.2008.02.012

mal incidence monochromator [14]. The energy calibration of the monochromator was performed using an intense and sharp CO_2 absorption peak at 16.48 eV [15]. A LiF filter was used in the energy range below 11 eV in order to remove the higher order energies from diffraction grating. A GaAs photodiode located behind the interaction region was used to normalize the ion yield spectra to the flux of the monochromatized light. The spectra were corrected also for the quantum efficiency of the photodiode [16].

At home laboratory in Oulu the experiments were carried out with two excitation methods, 500 eV electrons and HeI photons. 500 eV electron beam with 40 μA current was produced by SPECS electron gun EQ 22/35. HeI excitation (21.22 eV) was produced by SPECS UVS 300 UV lamp.

The experimental setup consists of a vacuum chamber equipped with the home made Wiley–McLaren time-of-flight mass spectrometer [17,18]. The TOF spectrometer consists of the 300 mm free drift length ion analyzer where ions are detected by multichannel plate (MCP) detector in the Chevron configuration. Calibration of TOF apparatus was done with Ar and Xe noble gases. The uncertainty of the time-of-flight experiments comes from variations of pressure, photon flux and mainly from the MCP and photodiode efficiency, especially for the low photon energy where background is high. It gives an estimated experimental error limit of 7% for the total ion yield. For the partial ion yield of the individual fragments the relative error is linearly increased and reaches 30% for the minor fragments below 2% from total ion yield.

During partial ion yield (PIY) experiments the photon energy was changed from 9 to 25 eV with a step of 0.15 eV and 15 s accumulation time. Branching ratio for each fragment was calculated from partial ion yield of the fragment divided by the total ion yield. The liquid sample TBT chloride (96%, Aldrich) was kept in a vacuum reservoir at room temperature and delivered to interaction region in vapour phase by gas line. The pressure in the experimental chamber was in a range of 10^{-7} mbar during the measurements.

3. Calculations

Theoretical calculations were performed using GAMESSsoftware package [19,20]. The geometry optimization was run assuming a C_{3v} symmetry with the Sn and the Cl atoms on the principal axis and using the butane molecule (C_4H_{10}) with a missing hydrogen as starting geometry for the (C_4H_9) groups. For the geometry optimization and the electronic structure analysis of the molecule a DFT approach [21] with Slater type STO-3G [22–24] basis set was used. More specifically, local spin density approximation (LSDA) [25] calculations that combine Slater exchange and VWN correlation, a method also referred to as SVWN, have been carried out.

4. Results and discussion

The structural formula of the TBTCl molecule is shown in Fig. 1a. Bond lengths Sn–C and Sn–Cl are 2.08 Å and 2.31 Å, respectively, according to geometry optimization calculations, and the angles C–Sn–C and Cl–Sn–C are 114.2° and 107.1°, respectively. The Mulliken and Lodwin population analysis revealed a partial negative charge on the Cl atom (∼ −0.3e) and a partially positive charge (∼ +0.8e) on the Sn atom. Each $(C_4H_9)_3$ group revealed an overall partial negative charge (∼ −0.16e) with the C atoms being partially negatively charged and with the carbon atoms directly bounded to the Sn atom retaining the largest partially negative charge (∼ −0.33e).

Fig. 1b shows the time-of-flight spectra of TBTCl when the molecule is ionized by photons with energies of 9 eV (a), 9.5 eV (b), 14 eV (c), 20 eV (d) and 25 eV (f) from the synchrotron, by photons from a HeI lamp (e) and by 500 eV electrons (g). Nine fragments:

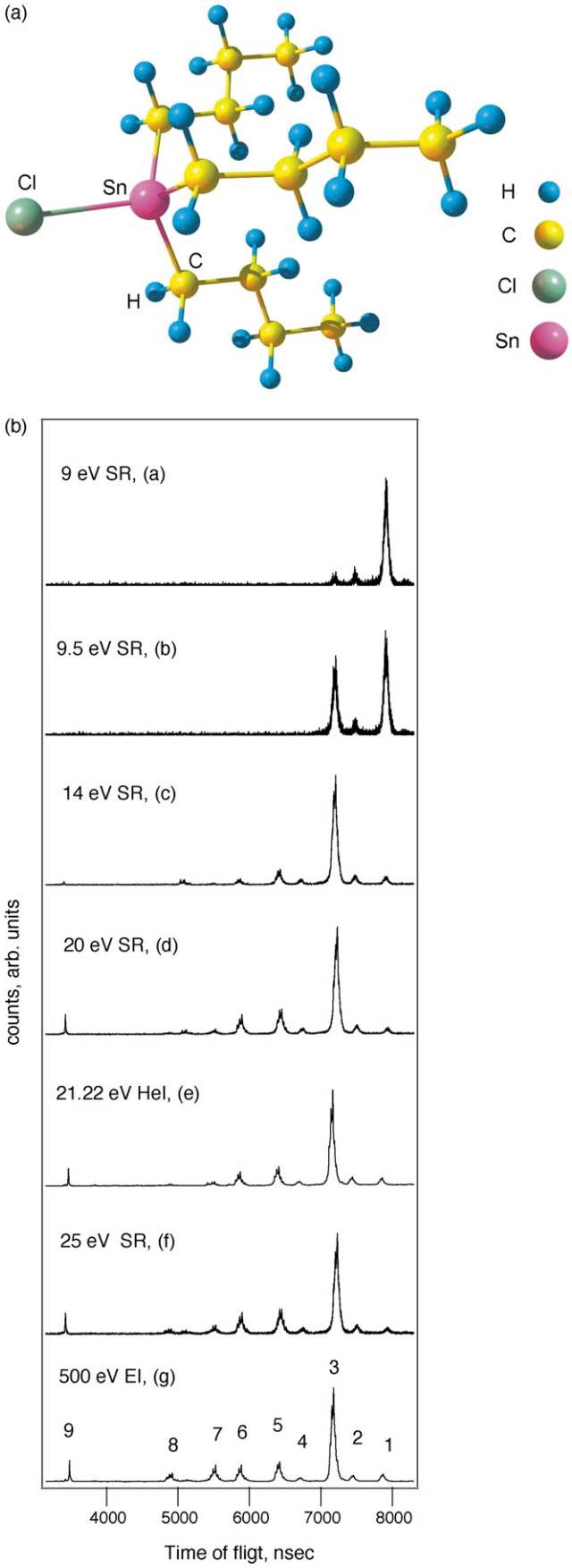

Fig. 1. (a) Tributyltin chloride $(C_4H_9)_3SnCl$ molecule. For details, see text. (b) Time-of-flight spectra of TBTCl excited using synchrotron radiation (SR) with photon energies of 9, 9.5, 14, 20 and 25 eV, with HeI (21.22 eV) and 500 eV electrons (EI). For assignment of the fragments 1–9 see Table 1.

Table 1
Ratios of the TBTCl fragments after ionization by synchrotron radiation (SR), HeI and electron beam (EI)

Fraction	SR (9 eV, %)	SR (9.5 eV,%)	SR (14 eV, %)	SR (20 eV, %)	HeI (21.22 eV, %)	SR (25 eV, %)	EI (500 eV, %)
1. $C_{12}H_{27}SnCl$	77.6	49.3	5.6	4.9	4.7	4.5	4.2
2. $C_{12}H_{27}Sn$	13.1	8.5	6.0	5.0	4.9	5.0	3.2
3. $C_8H_{18}SnCl$	9.3	42.2	77.3	63.4	61.9	57.9	53.3
4. $C_8H_{18}Sn$	–	–	1.7	2.4	2.5	2.5	2.1
5. C_4H_9SnCl	–	–	7.8	12.2	12.6	11.7	12.1
6. C_4H_9Sn	–	–	1.6	8.2	8.4	9.5	8.7
7. SnCl	–	–	–	1.8	2.3	4.1	8.9
8. Sn	–	–	–	0.5	0.9	2.4	4.6
9. C_4H_9	–	–	0.0	1.7	1.8	2.4	2.9

The estimated experimental error limit is 7% for the total ion yield and error is linearly increased and reaches 30% for partial yields of the minor fragments below 2%.

tributyltin chloride (1, TBTCl, $(C_4H_9)_3SnCl$), tributyltin (2, TBT, $(C_4H_9)_3Sn$), dibutyltin chloride (3, DBTCl, $(C_4H_9)_2SnCl$), dibutyltin (4, DBT, $(C_4H_9)_2Sn$), monobutyltin chloride (5, MBTCl, C_4H_9SnCl), monobutyltin (6, MBT, C_4H_9Sn), tin chloride (7, SnCl), tin (8, Sn) and butyl (9, C_4H_9) were detected. The fragments which contain tin atom have fine structure broadening corresponding to the natural abundance of the Sn isotopes. The relative amounts of the fragments obtained at various excitation energies are presented in Table 1. Previous results obtained using the gas chromatography–electron ionization–mass spectrometry [13] are in a good agreement with our experiments taken with electron beam excitation. Results taken with photon energy of 21.22 eV are the same both in HeI and synchrotron radiation excited spectra within the experimental accuracy. During the experiments the energy of the electron gun was changed to 1000 eV and 1500 eV, but this did not change the relative amount of fragments more than 0.5% if compared with 500 eV electron beam excitation, which shows saturation in dissociation of the TBT chloride.

Fig. 2 shows partial ion yields of TBTCl fragment ions at the photon energy range of 9–25 eV. Below 9 eV the main fragment ion (more than 90%) is $TBTCl^+$, but at the photon energy range of 10–25 eV the dominating fragment ion (above 50%) is $DBTCl^+$. At photon energy range of 12–25 eV the $DBTCl^+$ ions dissociate further to smaller fragments. The Sn^+, $SnCl^+$ and $butyl^+$ yields show linear dependence from the photon energy, and their yields do not reach saturation at 25 eV. As seen from Table 1, the production of Sn^+ and $SnCl^+$ ions depends strongly on the ionization energy. According to the calculations, there are several atoms within the 0–25 eV ionization energy (IE) range that are affected by the photoionization process. Fig. 3 presents the IE diagram for the TBTCl molecule. The smallest IEs involve molecular orbitals (MO) whose main components are the valence orbitals of the C and Sn atoms. At higher IE the Cl and the Sn atomic orbitals (AO) start to play a bigger role in the corresponding MO.

In the IE range up to 4.0 eV, the MOs are mainly characterized by the outermost valence orbitals of atoms, mainly C2p, Sn5p and H1s. It is unlikely that the ionization of these delocalized orbitals destabilizes the structure of the ionized molecule that indeed is present as $(C_4H_9)_3SnCl^+$ in the TOF spectrum measured with photon energy of 9 eV shown in Fig. 1b. At higher photoionization energies, the MO e and a_1 were found at 6.6 eV with strong Cl3p AO character and a_1 at 8.8 eV with strong Cl3s AO character. A photoionization of these orbitals most likely causes a fragmentation of the ionized molecule as follows:

$$(C_4H_9)_3SnCl^+ \rightarrow (C_4H_9)_3Sn^+ + Cl^0$$

In this process, the more electronegative chlorine atom retains the valence electron and stays with an overall neutral charge. This would explain the presence of the $(C_4H_9)_3SnCl^+$ ion and the lack of Cl^+ ion in the TOF spectrum (a) (see Fig. 1b). From the TOF spectra (b) and (c) the drastic increase of the $(C_4H_9)_2SnCl^+$ signal for 9.5 eV photon energy and its almost exclusive presence for 14 eV match with the IE of the MO a_1 at 9.5–9.6 eV with strong C2s AO character and MO e and a_1 at 16.8 eV with strong Sn4d AO character. In this case the fragmentation process following the photoionization can be described as follow:

$$(C_4H_9)_3SnCl^+ \rightarrow (C_4H_9)_2SnCl^+ + (C_4H_9)^0$$

The split of the molecule most likely resembles the one described before for the Cl atom, where in this case it is the (C_4H_9) group that retains the valence electron and stays with an overall neutral charge. This explains also the lack of $(C_4H_9)^+$ signal in the spectrum (b) (see also Table 1). For 14 eV photon energy we probably start to reach the Sn4d orbitals and the fragmentation process is as follow:

$$(C_4H_9)_3SnCl^+ \rightarrow (C_4H_9)_2SnCl^0 + (C_4H_9)^+$$

or

$$(C_4H_9)_3SnCl^+ \rightarrow (C_4H_9)_2SnCl^+ + (C_4H_9)^+ + e^-$$

Indeed at these energies a weak signal from the $(C_4H_9)^+$ is observed. The second decay includes the possibility that a deep photoionization triggers a non-radiative decay with the emission of an Auger electron and with the production of two ionized molecules.

For higher (24.5–27.3 eV) IE the MO are mainly a_1 with strong Sn4s AO character and e, a_1 with strong Sn4p AO character. The main fragmentation products are still the same as seen from the measured TOF spectra (d–f), but there is a growing strength of the $(C_4H_9)_2Sn^+$, $(C_4H_9)SnCl^+$ and $(C_4H_9)Sn^+$ signals. This can be a consequence of several possible decay pathways: at these photon energies the ionization occurs at deeper orbitals and the fragmentation process implies a non-radiative decay, but with the production of several fragments, all except one with an overall neutral charge undetectable. In order to follow in detail these processes further work is needed, possibly using coincidence (PIPECO) experiments that would allow the detection of each product with the emission of the Auger electron.

Because of the nature of the ionization process using electron beam, the TOF spectrum shown in Fig. 1b shows almost all the peaks described above (see also Table 1). Using an electron beam of 500 eV allowed us to ionize the molecule from even deeper orbitals, mainly from the MO a_1 (99 eV) with strong Cl2s AO character, MO a_1 with strong Sn3s AO character and MO e and a_1 with strong Sn3p AO character and the strength of the $SnCl^+$ and Sn^+ signal increase in the TOF spectrum (g).

In respect to environmental studies, if we take into account that the energy of the solar light on the Earth is mainly in the energy range of 0–5 eV [26] the photofragmentation of the TBTCl described above is unlikely. Present experiments were, however, limited in the low photon energy region above 9 eV. At lower photon energies resonant excitation instead of ionization may take place. If such valence excited states result in the fragmentation of TBTCl, it has to be investigated separately. Beam line at MAX-III, under commis-

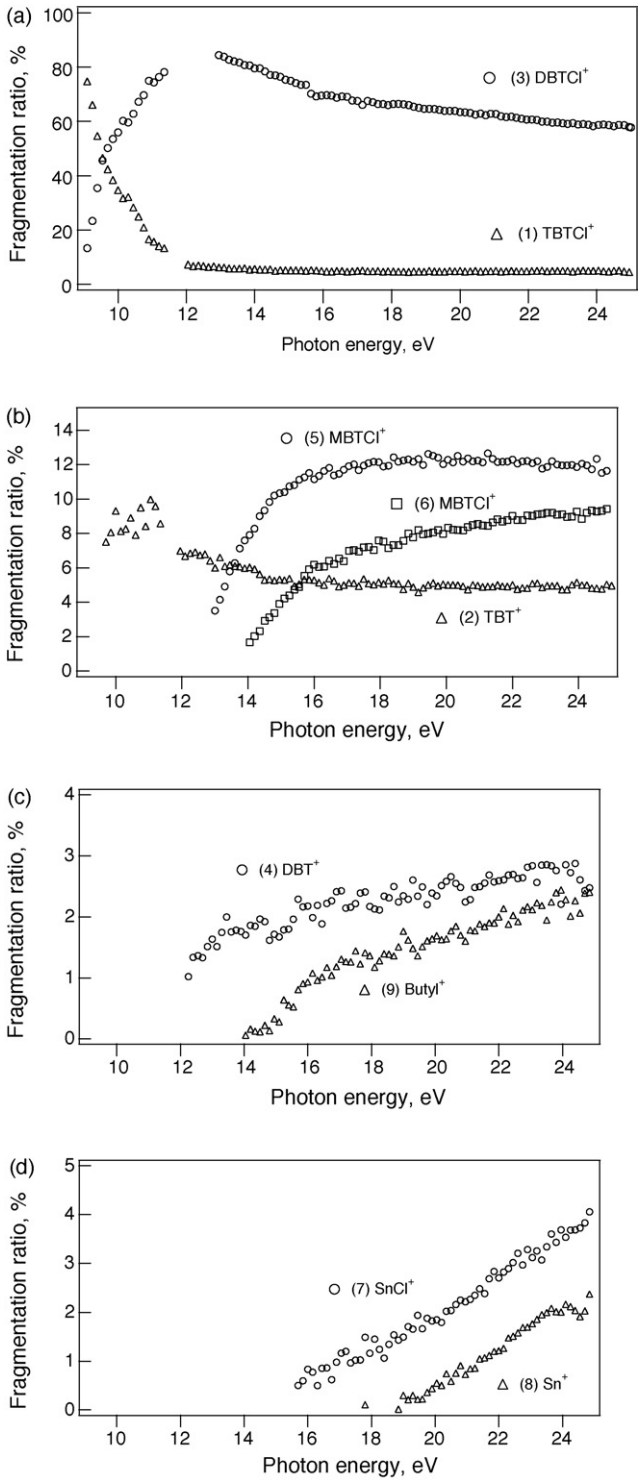

Fig. 2. Partial ion yields of the TBTCl fragments at the photon energy region of 9–25 eV.

sioning at the moment, would offer excellent possibilities for such studies.

Our results taken at the photon energy of 9 eV, which are the closest in the energy to the solar light, give lower TBTCl fragmentation than the results taken with HeI and electron ionization where dissociation of TBTCl is very high. On the other hand, most spectroscopic tools applied in the analysis of organotin concentrations in the environment use laboratory sources to create the photoelectric effect, which may create fragmentation of the TBT molecule as seen

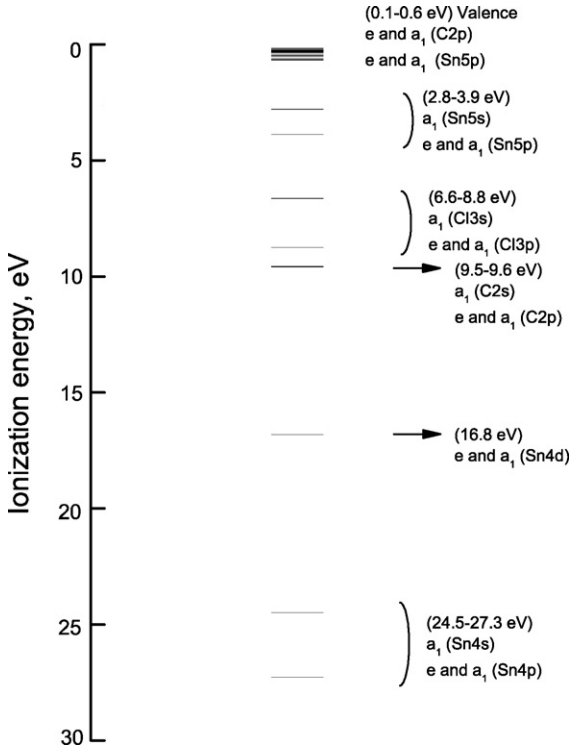

Fig. 3. Ionization energy diagram in the energy range of 0–30 eV for TBTCl molecule. Notes on right side show corresponding energies for molecular orbitals (with main atomic orbital character).

above. In conclusion, energy dependence of spectroscopic analytical methods was demonstrated in detail. In addition, comparison between experiment and calculations made it possible, for the first time, to follow the fragmentation dynamics of the TBT compound.

Acknowledgements

We are grateful to the staff of the MAX laboratory and to M. Remes for their help during the measurements and to T. Takaluoma for helpful discussions. Financial support from the Research Council for Natural Science and Technology of the Academy of Finland is acknowledged. The work was also supported by European Community - Research Infrastructure Action under the FP6 "Structuring the European Research Area" Program (through the Integrated Infrastructure Initiative "Integrating Activity on Synchrotron and Free Electron Laser Science").

References

[1] M. Hoch, Appl. Geochem. 16 (2001) 719.
[2] Y. Takahashi, N. Sakakibara, M. Nomura, Anal. Chem. 76 (2004) 4307.
[3] K. Newman, R.S. Mason, J. Anal. At. Spectrom. 20 (2005) 830.
[4] P. Visoottiviseth, K. Kruawan, A. Bhumiratana, P. Wileirat, Appl. Organomet. Chem. 9 (1995) 1.
[5] A. Pain, J.J. Cooney, Arch. Environ. Contam. Toxicol. 35 (1998) 412.
[6] G.M. Gadd, Sci. Total Environ. 258 (2000) 119.
[7] M. Hoch, D. Schwesig, Appl. Geochem. 19 (2004) 323.
[8] R.J. Maguire, J.H. Carey, E.J. Hale, J. Agric. Food Chem. 31 (1983) 1060.
[9] M. Monperrus, O. Zuloaga, E. Krupp, D. Amouroux, R. Wahlen, B. Fairman, O.F.X. Donard, J. Anal. At. Spectrom. 18 (2003) 247.
[10] G. Centineo, P. Rodriguez-Gonzales, E.B. Gonzalez, J.I.G. Alonso, A. Sanz-Medel, J. Mass Spectrom. 39 (2004) 485.
[11] M.G. Ikonomou, M.P. Fernandez, T. He, D. Cullon, J. Chromatogr. A 975 (2002) 319.
[12] J. Meija, G. Centineo, J.I.G. Alonso, A. Sanz-Medel, J.A. Caruso, J. Mass Spectrom. 40 (2005) 807.
[13] C. Bancon-Montigny, P. Maxwell, L. Yang, Z. Mester, R.E. Sturgeon, J.W. Lam, J. Anal. At. Spectrom. 17 (2002) 1506.

[14] S.L. Sorensen, B.J. Olsson, O. Widlund, S. Huldt, S.-E. Johansson, E. Källne, A.E. Nilsson, R. Hutton, U. Litzén, A. Svensson, Nucl. Instrum. Meth. Phys. Res. A 297 (1990) 296.
[15] D.A. Shaw, D.M.P. Holland, M.A. Hayes, M.A. MacDonald, A. Hopkirk, S.M. McSweeney, Chem. Phys. 198 (1995) 381.
[16] M. Krumrey, E. Tegeler, J. Barth, M. Krisch, F. Schäfers, R. Wolf, Appl. Opt. 27 (1988) 4336.
[17] W.C. Wiley, I.H. McLaren, Rev. Sci. Instrum. 26 (1955) 1150.
[18] M. Huttula, M. Harkoma, E. Nõmmiste, S. Aksela, Nucl. Instrum. Meth. Phys. Res. A 467–468 (2001) 1514.
[19] M.W. Schmidt, K.K. Baldridge, J.A. Boatz, S.T. Elbert, M.S. Gordon, J.H. Jensen, S. Koseki, N. Matsunaga, K.A. Nguyen, S. Su, T.L. Windus, M. Dupuis, J.A. Montgomery Jr., J. Comput. Chem. 14 (1993) 1347.
[20] M.S. Gordon, M.W. Schmidt, C.E. Dykstra, G. Frenking, K.S. Kim, G.E. Scuseria, Theory and Applications of Computational Chemistry, The First Forty Years, Elsevier, Amsterdam, 2005.
[21] R.G. Parr, W. Yang, Density Functional Theory of Atoms and Molecules, Oxford Scientific, 1989.
[22] W.J. Hehre, R.F. Stewart, J.A. Pople, J. Chem. Phys. 51 (1969) 2657.
[23] W.J. Hehre, R. Ditchfield, R.F. Stewart, J.A. Pople, J. Chem. Phys. 52 (1970) 2769.
[24] W.J. Pietro, E.S. Blurock, R.F. Hout, W.J. Hehre, D.J. DeFrees, R.F. Stewart Jr., Inorg. Chem. 20 (1981) 3650.
[25] S.H. Vosko, L. Wilk, M. Nusair, Can. J. Phys. 58 (1980) 1200.
[26] J.T. Kiehl, K.E. Trenberth, Bull. Am. Meteorol. Soc. 78 (1997) 197.